Ionization Dynamics in Laser Irradiated Matter Doped with Nanoantennas for NAPLIFE project

István Papp, [1,2], Konstantin Zhukovsky [1,3]
(part of NAPLIFE Collaboration)

[1] Wigner HUN-REN Research Centre for Physics, Budapest,
[2] HUN-REN Centre for Energy Research, Budapest,
[3] Department of Theoretical Physics, Faculty of Physics, M.V.Lomonosov Moscow State University, Moscow

GPU Workshop Wigner RCP, May 31, 2024, Budapest

Nanoplasmonic Laser Fusion Research Laboratory

Host Institute: Wigner FK
Director General: Lévai Péter
Finance: Vámos-Szigeti Klára

Project scientific leader:
Bíró Tamás Sándor (Wigner FK)

Project manager:
Szeledi Anett (Wigner FK)

Book-keeping:
Dömötör Antónia (Wigner FK)

Project Governing Body:
Szabó Gábor (ELI-ALPS), chair
Varga Dezső (WFK), secretary
Czitrovszky Aladár (WFK),
Nagy Attila (WFK),
Szabó István (NKFIH)

Science advisors:
Kroó Norbert, prof. em. (Wigner FK) Csernai László, prof. em. (Uni.Bergen)

Theory Group:
Csete Mária (SZTE)
Papp István (Wigner FK)
Tóth Emese (SZTE)
Vass Dávid (SZTE)
Szenes András (SZTE)
Bánhelyi Balázs (SZTE)
Czirják András (SZTE)
Földi Péter (SZTE)

Nanotechnology Group:
Bonyár Attila (BME ETT)
Borók Alexandra (BME ETT)
Szalóki Melinda (DE FOK)
Petrik Péter (EK)
Schereen Zangana (BME)

Laser Group:
Rácz Péter (Wigner FK)
Dombi Péter (Wigner FK)
Kedves Miklós (Wigner FK)
Aladi Márk (Wigner FK)
Kumari Archana (Wigner FK)

Spectroscopy Group:
Veres Miklós (Wigner FK)
Rigó István (Wigner FK)
Nagyné Szokol Ágnes (Wigner FK)
Holomb Román (Wigner FK)
Kámán Judit (Wigner FK)
Galbács Gábor (SZTE)

Thermo-nuclear Fusion

- ηE_f is the usable energy
- The loss is $(1-\eta)(E_0 + E_b)$
- $E_0 = 3nkT$, $E_b = bn^2\tau\sqrt{T}$ (thermal bremsstralung)
- Giving the gain factor: $Q = \frac{\eta\epsilon n\tau v\sigma}{4(1-\eta)(3kT+bn\tau\sqrt{T})}$
- Q must be $Q > 1$ for energy production
- This also means $n\tau > \frac{3kT(1-\eta)}{\frac{1}{4}\epsilon\eta\langle v\sigma\rangle - b(1-\eta)\sqrt{T}} \rightarrow$ LC

Lawson criterion

Fulfilling the Lawson criterion

- Magnetically confined plasmas: increase confinement time
- Inertial confinement fusion: increase density of fusion plasma

News on fusion

Quasi-IsoDynamic Stellarator

first light

HB11 ENERGY
LASER BORON FUSION

National Ignition Facility LLNL first year of sooting

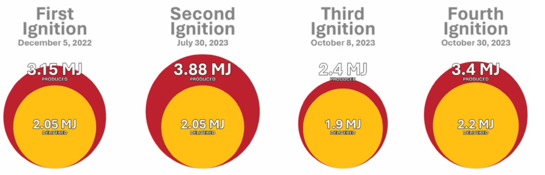

LLNL has achieved fusion ignition on NIF four times to date. Credit: Brian Chavez

Direct vs Indirect drive

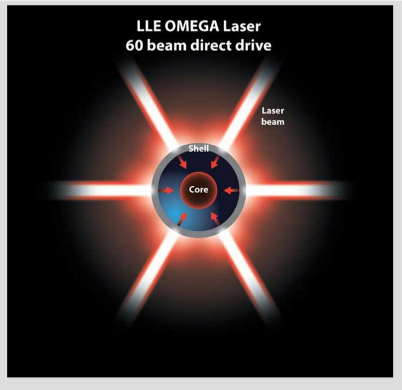

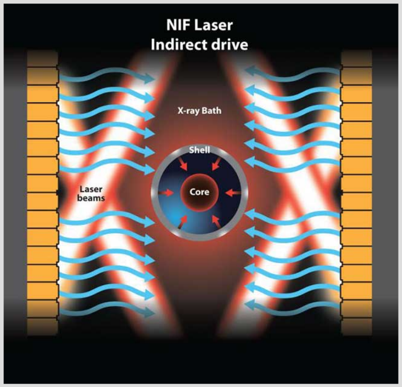

PHOTONICS MEDIA photonics.com

Hohlraum 2014

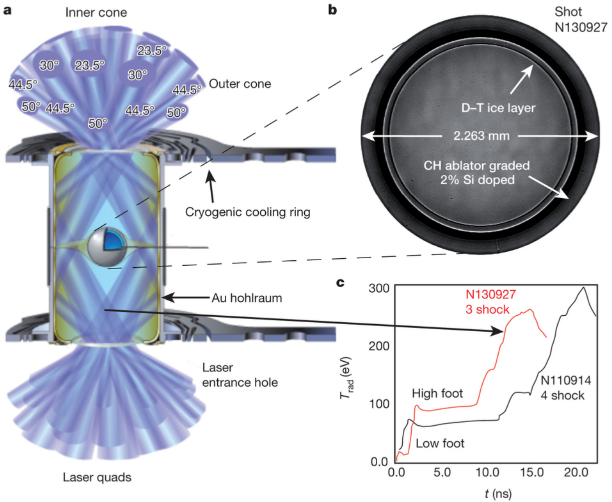

[O.A. Hurricane et al., Nature, 506, 343 (2014)]

Hohlraum 2022

Fig. 1: Schematic of the indirect-drive inertial confinement approach to fusion.

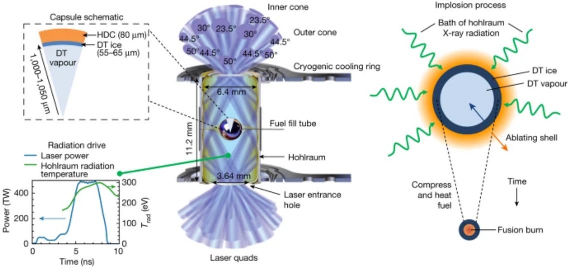

Centre, A typical indirect-drive target configuration with key engineering elements labelled. Laser beams (blue) enter the hohlraum through laser entrance holes at various angles. Top left, A schematic pie diagram showing the radial distribution and dimensions of materials in diamond (high-density carbon, HDC) ablator implosions. Bottom left, The temporal laser power pulse-shape (blue) and associated hohlraum radiation temperature (green). Right, At the centre of the hohlraum, the capsule

[A.B, Zylstra, O.A. Hurricane et al., Nature, 601, 542-548 (2022)]

NIF older | newer target

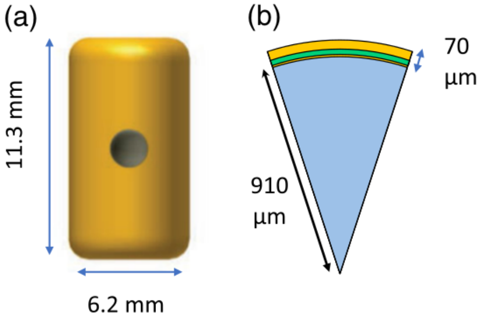

- thin plastic ablator | tungsten-doped diamond-like high density carbon
- gold hohlraum | depleted uranium hohlraum

Rayleigh-Taylor instabilities

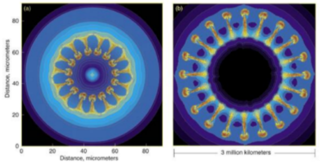

Striking similarities exist between hydrodynamic instabilities in (a) inertial confinement fusion capsule implosions and (b) core-collapse supernova explosions. [Image (a) is from Sakagami and Nishihara, *Physics of Fluids B* **2**, 2715 (1990); image (b) is from Hachisu et al., *Astrophysical Journal* **368**, L27 (1991).]

Energy must be delivered as sysmmetric as possible!

Different levels of corrugation of the shell surfaces :

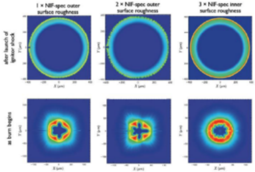

Left: same roughness of inner and outer surface as specified for the NIF target
Center: outer surface roughness is twice the NIF level
Right: DT inner surface roughness three times larger than NIF specifications

[S. Atzeni et al., Nucl. Fusion 54, 054008 (2014).] 25

Latest (January 2023) news 3.15MJ kinetic energy at NIF with burning time of 89-137 ps(?)

Relativistic Fluid Dynamics

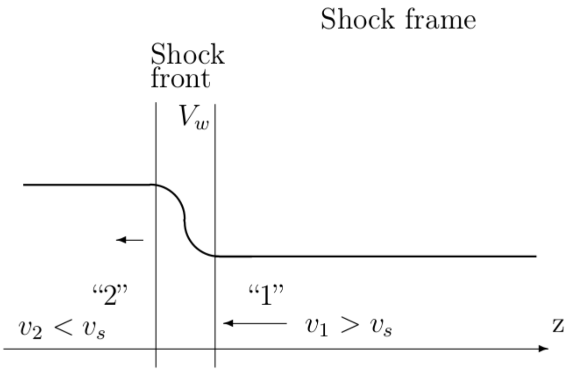

[Csernai, L.P. (1987). Detonation on a time-like front for relativistic systems. Zh. Eksp. Teor. Fiz. 92, 379-386.]

Relativistic Fluid Dynamics

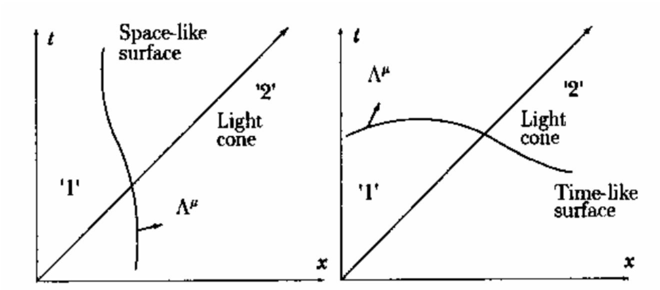

Figure 5.9: Space-like (a) and time-like (b) surfaces of discontinuity

[Csernai, L.P. (1987). Detonation on a time-like front for relativistic systems. Zh. Eksp. Teor. Fiz. 92, 379-386.]

Relativistic Fluid Dynamics

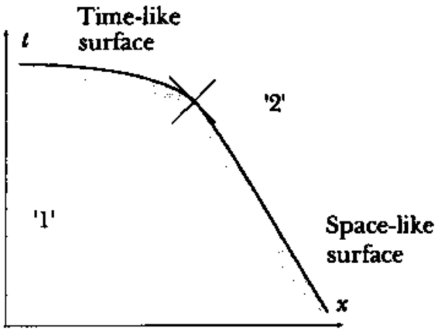

Figure 5.10: Smooth change from spacelike to timelike detonation

[Csernai, L.P. (1987). Detonation on a time-like front for relativistic systems. Zh. Eksp. Teor. Fiz. 92, 379-386.]

Constant absorptivity

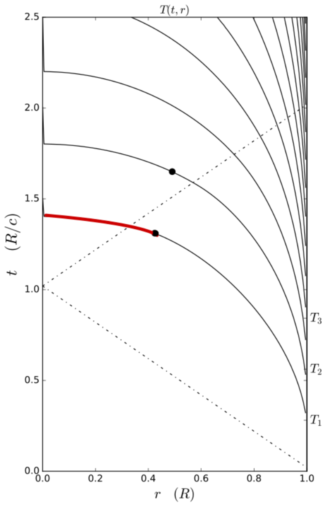

[L.P. Csernai & D.D. Strottman, Laser and Particle Beams 33, 279 (2015)]

$\alpha_{k_{middle}} = \alpha_{k_{edge}}$

Simultaneous volume ignition is only up to 12%

Changing absorptivity

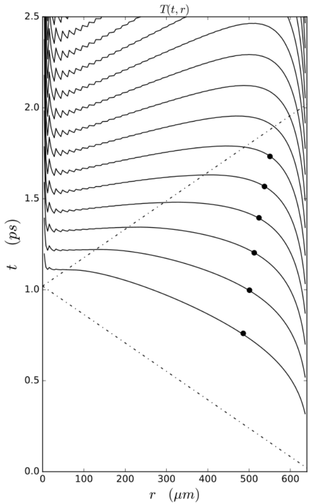

[Csernai, L.P., Kroo, N. and Papp, I. (2017). Procedure to improve the stability and efficiency of laser-fusion by nano-plasmonics method. Patent P1700278/3 of the Hungarian Intellectual Property Office.]

$\alpha_{k_{middle}} \approx 4 \times \alpha_{k_{edge}}$

Simultaneous volume ignition is up to 73%

Flat target, two sided shot

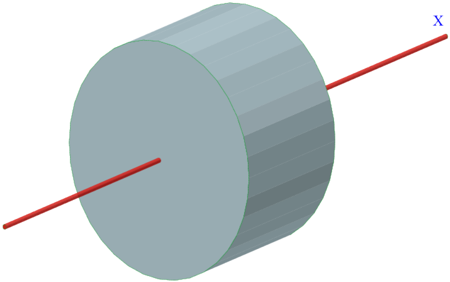

Schematic view of the cylindrical, flat target of radius, R, and thickness, h.
$V = 2\pi R^3, \quad R = \sqrt[3]{V/(2\pi)}, \quad h = \sqrt[3]{4V/\pi}.$

[L.P. Csernai, M. Csete, I.N. Mishustin, A. Motornenko, I. Papp, L.M. Satarov, H. Stöcker & N. Kroó, Radiation- Dominated Implosion with Flat Target, *Physics and Wave Phenomena*, **28** (3) 187-199 (2020)]

Varying absorptivity, similar configuration

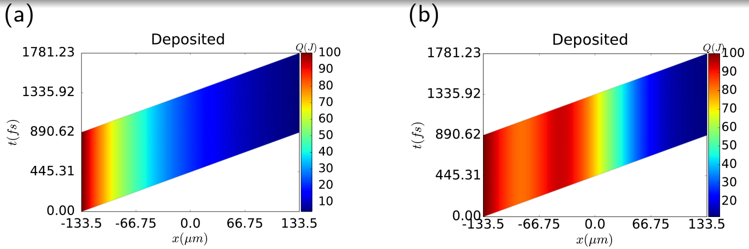

Deposited energy per unit time in the space-time plane across the depth, *h*, of the flat target. **(a) without** nano-shells **(b) with** nano-shells

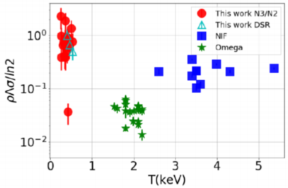

Nuclear probes of an out-of-equilibrium plasma at the highest compression **Phys. Lett. A 383 (2019) 2285-2289.**

G. Zhang [a,b,*], M. Huang [c], A. Bonasera [d,e,*], Y.G. Ma [f,b,i,*], B.F. Shen [g,h,*], H.W. Wang [a,b], W.P. Wang [g], J.C. Xu [g], G.T. Fan [a,b], H.J. Fu [b], H. Xue [b], H. Zheng [j], L.X. Liu [a,b], S. Zhang [c], W.J. Li [b], X.G. Cao [a,b], X.G. Deng [b], X.Y. Li [b], Y.C. Liu [b], Y. Yu [g], Y. Zhang [b], C.B. Fu [k], X.P. Zhang [k]

Similar **two sided** shooting configuration was already scessful

Nanoplasmonic Laser Fusion Research Laboratory

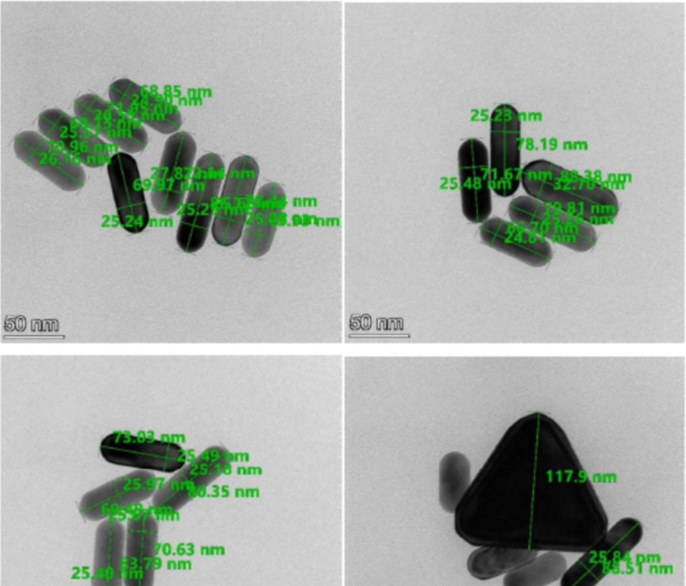

Transmission Electron-microscopy photos of 75x25 nm gold nano-rod antennas **[Judit Kámán, A. Bonyár** et al. (NAPLIFE Collab.)., Gold nanorods ..., 10th ICNFP 2021, **Kolymbari]**

Nanorod

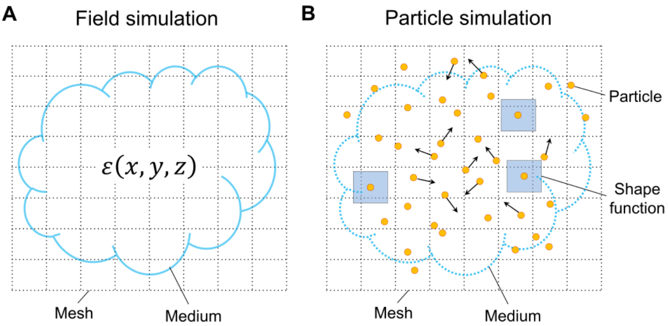

[W. J. Ding,et al., Particle simulation of plasmons Nanophotonics, vol. 9, no. 10, pp. 3303-3313 (2020)]

Particle In Cell methods

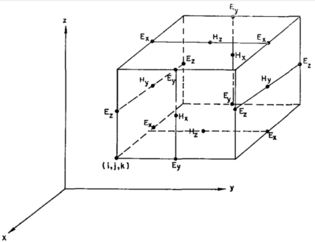

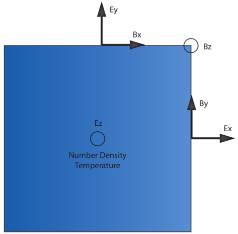

Figure 2: The Yee grid in 2D

[F.H. Harlow (1955). A Machine Calculation Method for Hydrodynamic Problems. Los Alamos Scientific Laboratory report LAMS-1956]

[T.D. Arber et al 2015 Plasma Phys. Control. Fusion 57 113001]

A **super-particle** (**marker-particle**) is a computational particle that represents many real particles.

Particle **mover** or **pusher** algorithm as (typically Boris algorithm).

Finite-difference time-domain method for solving the time evolution of **Maxwell's equations**.

Particle shape

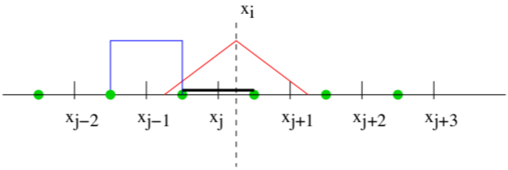

Figure 3: Second order particle shape function

First order approximations are considered

$$F_{part} = \frac{1}{2}F_{i-1}\left(\frac{1}{2} + \frac{x_i - X}{\Delta x}\right)^2 + \frac{1}{2}F_i\left(\frac{3}{4} - \frac{(x_i - X)^2}{\Delta x^2}\right)^2 + \frac{1}{2}F_{i+1}\left(\frac{1}{2} + \frac{x_i - X}{\Delta x}\right)^2$$

[EPOCH 4.0 dev manual]

FDTD in EPOCH

- $\boldsymbol{E}_{n+\frac{1}{2}} = \boldsymbol{E}_n + \frac{\Delta t}{2}\left(c^2\nabla\times\boldsymbol{B}_n - \frac{\boldsymbol{j}_n}{\epsilon_0}\right)$
- $\boldsymbol{B}_{n+\frac{1}{2}} = \boldsymbol{B}_n - \frac{\Delta t}{2}\left(\nabla\times\boldsymbol{E}_{n+\frac{1}{2}}\right)$
- Call particle pusher which calculates j_{n+1}
- $\boldsymbol{B}_{n+1} = \boldsymbol{B}_{n+\frac{1}{2}} - \frac{\Delta t}{2}\left(\nabla\times\boldsymbol{E}_{n+\frac{1}{2}}\right)$
- $\boldsymbol{E}_{n+1} = \boldsymbol{E}_{n+\frac{1}{2}} + \frac{\Delta t}{2}\left(c^2\nabla\times\boldsymbol{B}_{n+1} - \frac{\boldsymbol{j}_{n+1}}{\epsilon_0}\right)$

Particle pusher

- Solves the relativistic equation of motion under the Lorentz force for each marker-particle

$$\boldsymbol{p}_{n+1} = \boldsymbol{p}_n + q\Delta t \left[\boldsymbol{E}_{n+\frac{1}{2}} \left(\boldsymbol{x}_{n+\frac{1}{2}} \right) + \boldsymbol{v}_{n+\frac{1}{2}} \times \boldsymbol{B}_{n+\frac{1}{2}} \left(\boldsymbol{x}_{n+\frac{1}{2}} \right) \right]$$

  $\boldsymbol{p}$ is the particle momentum q is the particle's charge $\boldsymbol{v}$ is the velocity.
  $\boldsymbol{p} = \gamma m \boldsymbol{v}$, where m is the rest mass $\gamma = \left[(\boldsymbol{p}/mc)^2 + 1 \right]^{1/2}$
- Villasenor and Buneman current deposition scheme [Villasenor J & Buneman O 1992 Comput. Phys. Commun. 69 306], always satisfied: $\nabla \cdot \boldsymbol{E} = \rho/\epsilon_0$, where ρ is the charge density.

Metal Nanoparticles as Plasmas

The conduction band electrons in metals behave as strongly coupled plasmas.
For golden nanorods of 25nm diameter in vacuum this gives an effective wavelength of $\lambda_{eff} = 266\text{nm}$

$$\frac{\lambda_{eff}}{2R\pi} = 13.74 - 0.12[\varepsilon_\infty + 141.04] - \frac{2}{\pi} + \frac{\lambda}{\lambda_p} 0.12\sqrt{\varepsilon_\infty + 141.04}$$

[Lukas Novotny, Effective Wavelength Scaling for Optical Antennas, Phys. Rev. Lett. **98**, 266802 (2007).]

Ideal world: orthogonal to beam line

Nanorod inside a PIC simulation box

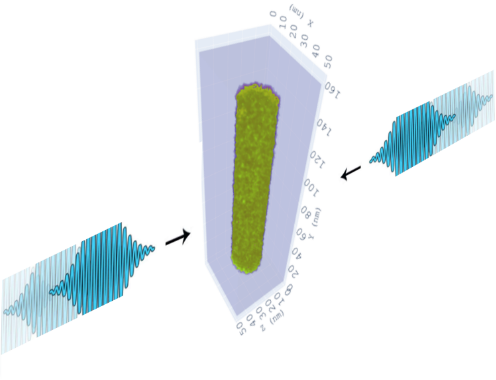

Evolution of the nanoantenna

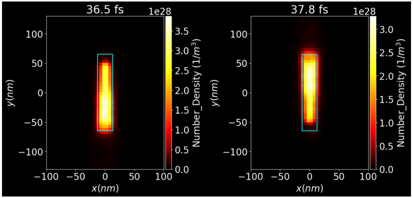

Number density of electrons in the middle of a nanorod of size 25x130 nm at different times. The nanorod is orthogonal to the beam direction, x.

Real world: scattered

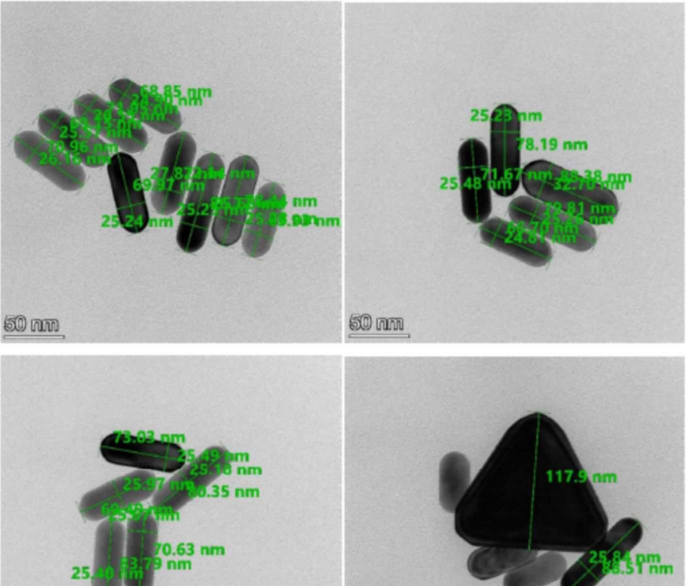

Transmission Electron-microscopy photos of 75x25 nm gold nano-rod antennas **[Judit Kámán, A. Bonyár** et al. (NAPLIFE Collab.)., Gold nanorods ..., 10th ICNFP 2021, **Kolymbari]**

Out of resonance (UDMA-TEGDMA copolymer)

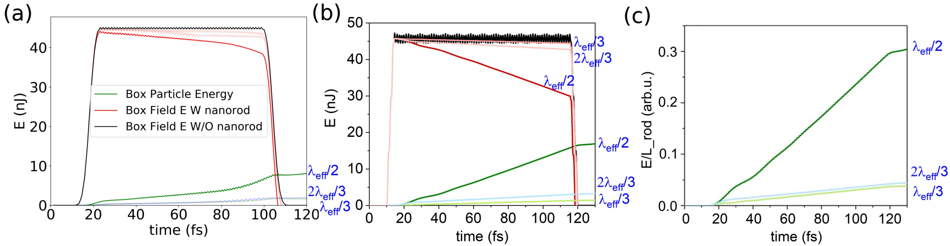

Optical response of the gold nanorod with different numerical methods and lengths, $L = \lambda_{eff}/2, \lambda_{eff}/3 and 2\lambda_{eff} eff/3$. (a) PIC, (b) FEM and (c) FEM with normalized values to unit antenna length.

[I. Papp, L. Bravina, M. Csete, et al.(NAPLIFE Collaboration), Kinetic model of resonant nanoantennas in polymer for laser induced fusion, Frontiers in Physics, **11**, 1116023 (2023).]

Comparing orientation, shapes and sizes

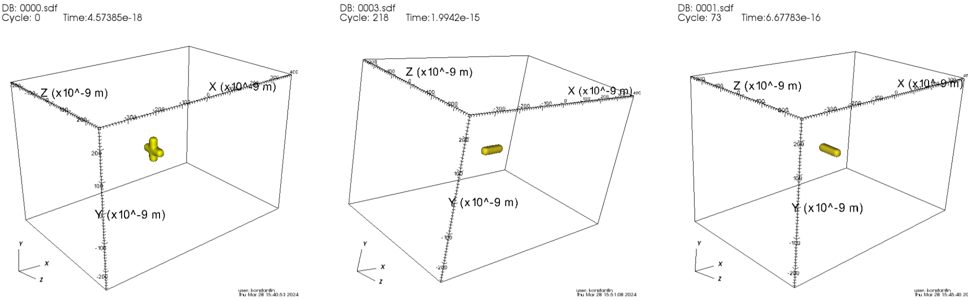

a b c

- We submerged the nanorods in Hydrogen medium
- Species were separately defined: conducting electrons, Au ions, H atoms, protons (H after ionized) and H electrons
- (a) **crossed** quadruple (b) **along** the beam direction (c) **laying** or sleeping policeman

Comparing orientation, shapes and sizes

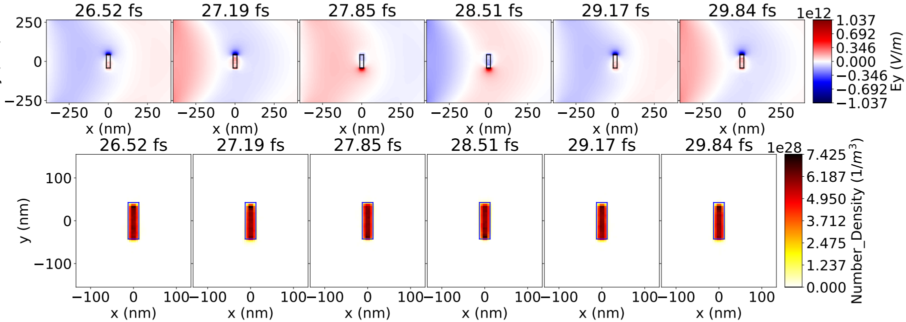

- Evolution of the E field's **polarization direction** component from 42.4 till 45.7 fs, around a nanorod of 25x85 nm. $I = 4 \cdot 10^{15}\text{W/cm}^2$
- Also side view of the proper conducting electron density of dipole oriented in **parallel** with polarization direction, in quarter of a period steps.

Comparing orientation, shapes and sizes

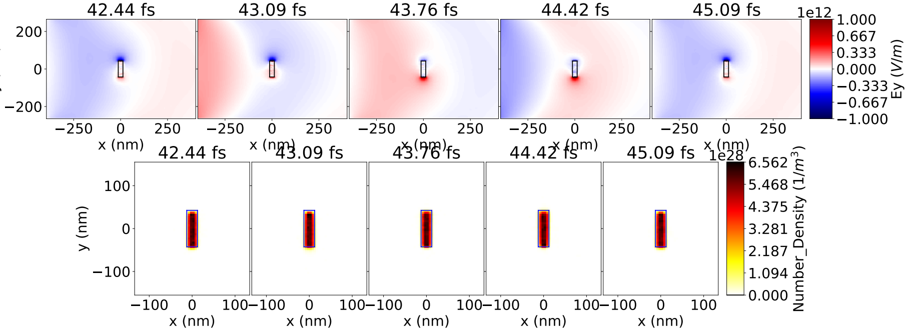

- Evolution of the E field's **polarization direction** component from 42.4 till 45.7 fs, around a **crossed quadroupole** (side view) of 25x85 nm. $I = 4 \cdot 10^{15}$W/cm^2
- Also side view of the proper conducting electron density in quarter of a period steps.

Comparing orientation, shapes and sizes

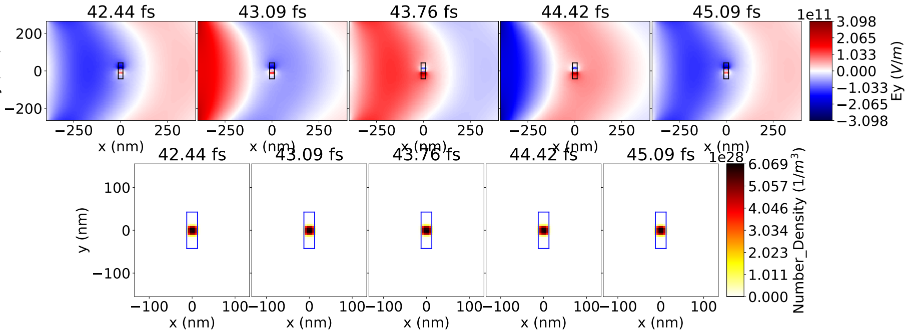

- Evolution of the E field's **polarization direction** component from 42.4 till 45.7 fs, around a "**laying**" sleeping police antenna of 25x85 nm. $I = 4 \cdot 10^{15} \mathrm{W/cm}^2$
- Also side view of the proper conducting electron density in quarter of a period steps. (Antenna is orthogonal to **both** polarization and beam direction).

Comparing orientation, shapes and sizes

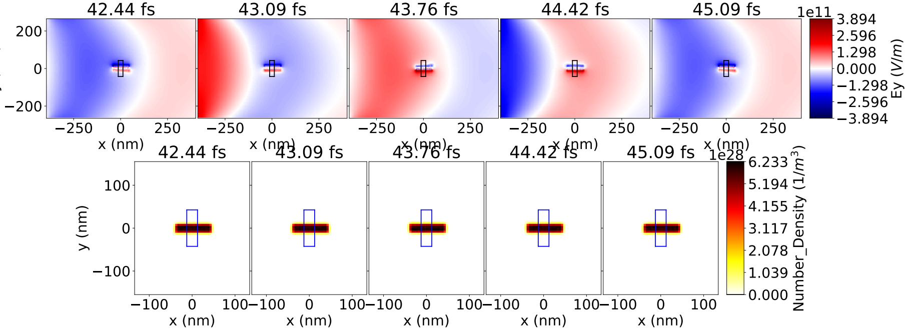

- Evolution of the *E* field's **polarization direction** component from 42.4 till 45.7 fs, around a nanorod of 25x85 nm. $I = 4 \cdot 10^{15}\mathrm{W/cm}^2$
- Also side view of the proper conducting electron density in quarter of a period steps. (Nanorod is parallel to the beam, orthogonal to the polarization).

Would spherical shapes be good then?

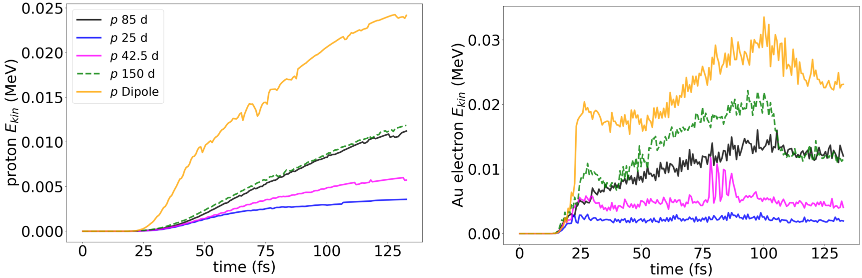

Time **evolution** of derived average **energies of** simulated ionized **Hydrogen** and **conducting electron** species of the gold nanodopes of spherical shape; diameters of dopes: 85 nm – black, 150 nm – green dashed, 42.5 nm – magenta, 25 nm – blue lines. Medium laser pulse intensities: 4×10^{15} W/cm^2 with 120 fs.

Cross checking

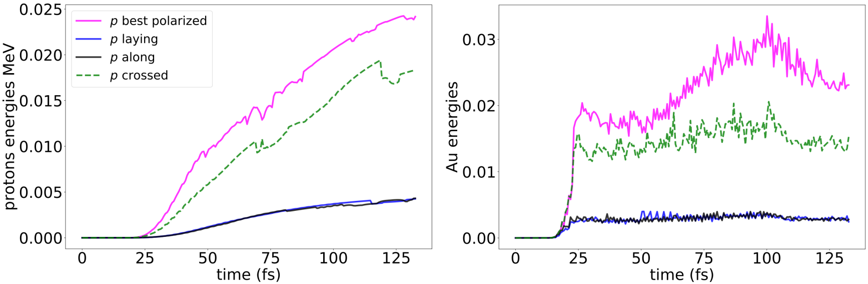

Time **evolution** of thr average **energies of** ionized **Hydrogen** and **conducting electron** species of gold nanodopes: crossed quadroupoles – green dashed, dipole of size 25x85 nm and ideal orientation along the field polarization – magenta, dipole laying across the field – blue, dipole along the pulse propagation – black lines. Medium laser pulse intensities: 4×10^{15} W/cm^2 with 120 fs.

Cross checking

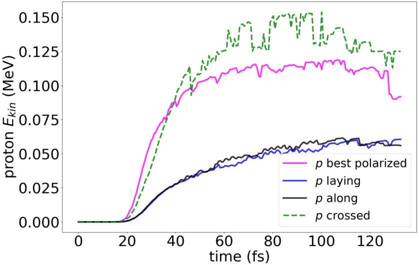

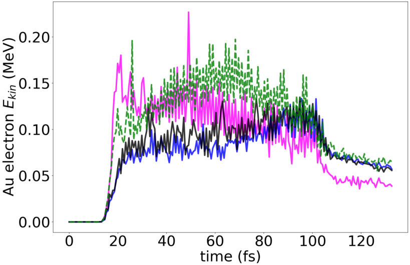

Time **evolution** of thr average **energies of** ionized **Hydrogen** and **conducting electron** species of gold nanodopes: crossed quadroupoles – green dashed, dipole of size 25x85 nm and ideal orientation along the field polarization – magenta, dipole laying across the field – blue, dipole along the pulse propagation – black lines. Medium laser pulse **intensities**: 4×10^{17} W/cm^2 with 120 fs.

Conclusions, Looking forward

- The model was proved to be in good agreement with currently available widely accepted methods, allowing us to confidently experiment further
- We compared various nanoantenna shapes, orientation and sizes
- Increasing radius of spherical nanoparticles increases the absorption but there is an apparent limit
- **Crossed quadruples** show advantageous behaviour irrespective of the orientation
- Crossed quadruples come close to the resonant dipoles, moreover at higher intensities can even perform **better**, which is promising for the **ELI-ALPS** experiments
- Further investigations will go to map the bet possibilites of target fabrication

Conclusions, Looking forward

Proton emmision from resonant targets

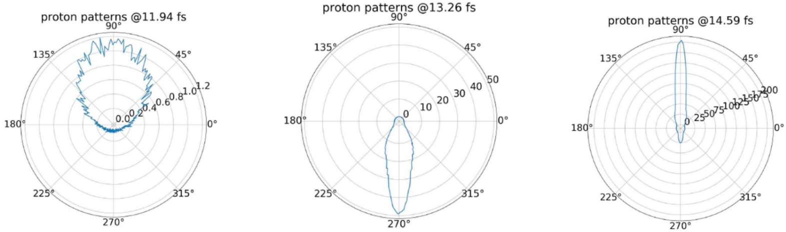

[Nuclear physics method to detect size, timespan and flow in nanoplasmonic fusion L.P. Csernai, T. Csörgő, I. Papp, M. Csete, András Szenes, Dávid Vass, T.S. Biró, N. Kroó; arXiv:2309.05156v3]

Conclusions, Looking forward

Conical rods

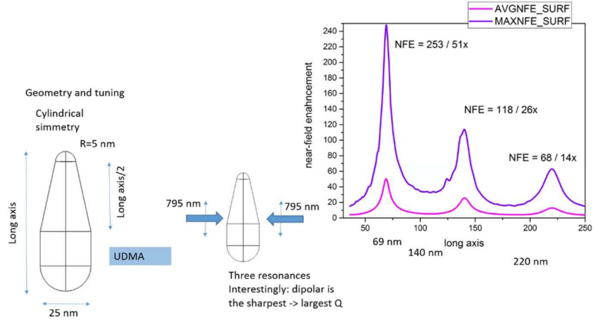

Expectation: **protons** can leave the asymmetric nano-rod antenna more at the **sharp edge** (like in case of lightening rods)
[J. Budai, Zs. Márton, M. Csete, 2024]

Acknoledgements

Enlightening discussions with Prof. Johann Rafelski are gratefully acknowledged. Horst Stöcker acknowledges the Judah M. Eisenberg Professor Laureatus chair at Fachbereich Physik of Goethe Universität Frankfurt. We would like to thank the **Wigner GPU Laboratory** at the Wigner Research Center for Physics for providing support in computational resources. This work is supported in part by the Frankfurt Institute for Advanced Studies, Germany, the Eötvös Loránd Research Network of Hungary, the Research Council of Norway, grant no. 255253, and the National Research, Development and Innovation Office of Hungary, via the projects: Nanoplasmonic Laser Inertial Fusion Research Laboratory (NKFIH-468-3/2021), Optimized nanoplasmonics (K116362), and Ultrafast physical processes in atoms, molecules, nanostructures and biological systems (EFOP-3.6.2-16-2017-00005). LP acknowledges support from Wigner RCP, Budapest (2022-2.2.1-NL-2022-00002).

We also greatly acknowledge **your** attention!